



Research article

Prediction of bacterial functional diversity in clay microcosms

Alexander A. Grigoryan^{a,b}, Daphne R. Jaliq^{a,c}, Simcha Stroes-Gascoyne^a,
Gideon M. Wolfaardt^{d,e}, Peter G. Keech^f, Darren R. Korber^{a,*}^a Department of Food and Bioproducts Sciences, University of Saskatchewan, Saskatoon, Canada^b Saudi Arabian Oil Company, Dhahran, Saudi Arabia^c Lallemand Inc., Saskatoon, Canada^d Department of Chemistry and Biology, Ryerson University, Toronto, Ontario, Canada^e Department of Microbiology, University of Stellenbosch, Cape Town, South Africa^f Nuclear Waste Management Organization, Toronto, Canada

ARTICLE INFO

Keywords:

Bentonite microcosms

Bacterial diversity

High-throughput sequencing

QIIME (quantitative insights into microbial ecology)

PICRUST (phylogenetic investigation of communities by reconstruction of unobserved states)

Potential bacterial activity

ABSTRACT

Microorganisms in clay barriers could affect the long-term performance of waste containers in future deep geological repositories (DGR) for used nuclear fuel through production of corrosive metabolites (e.g., sulfide), which is why clay materials are highly compacted: to reduce both physical space and access to water for microorganisms to grow. However, the highly compacted nature of clays and the resulting low activity or dormancy of microorganisms complicate the extraction of biomarkers (i.e., PLFA, DNA etc.) from such barriers for predictive analysis of microbial risks. In order to overcome these challenges, we have combined culture- and 16S rRNA gene amplicon sequencing-based approaches to describe the functional diversity of microorganisms in several commercial clay products, including two different samples of Wyoming type MX-80 bentonite (Batch 1 and Batch 2), the reference clay for a future Canadian DGR, and Avonlea type Canapril, a clay sample for comparison. Microorganisms from *as-received* bentonites were enriched in anoxic 10% w/v clay microcosms for three months at ambient temperature with addition of 10% hydrogen along with presumable indigenous organics and sulfate in the clay. High-throughput sequencing of 16S rRNA gene fragments indicated a high abundance of Gram-positive bacteria of the phylum Firmicutes (82%) in MX-80 Batch 1 incubations. Bacterial libraries from microcosms with MX-80 Batch 2 were enriched with Firmicutes (53%) and Chloroflexi (43%). Firmicutes also significantly contributed (<15%) to the bacterial community in Canapril clay microcosm, which was dominated by Gram-negative Proteobacteria (>70%). Sequence analysis revealed presence of the bacterial families *Peptostreptococcaceae*, *Clostridiaceae*, *Peptococcaceae*, *Bacillaceae*, *Enterobacteriaceae*, *Veillonellaceae*, *Tissierellaceae* and *Planococcaceae* in MX-80 Batch 1 incubations; *Bacillaceae*, along with unidentified bacteria of the phylum Chloroflexi, in MX-80 Batch 2 clay microcosms, and *Pseudomonadaceae*, *Hydrogenophilaceae*, *Bacillaceae*, *Desulfobacteraceae*, *Desulfobulbaceae*, *Peptococcaceae*, *Pelobacteraceae*, *Alcaligenaceae*, *Rhodospirillaceae* in Canapril microcosms. Exploration of potential metabolic pathways in the bacterial communities from the clay microcosms suggested variable patterns of sulfur cycling in the different clays with the possible prevalence of bacterial sulfate-reduction in MX-80 bentonite, and probably successive sulfate-reduction/sulfur-oxidation reactions in Canapril microcosms. Furthermore, analysis of potential metabolic pathways in the bentonite enrichments suggested that bacteria with acid-producing capabilities (i.e., fermenters and acetogens) together with sulfide-producing prokaryotes might perhaps contribute to corrosion risks in clay systems. However, the low activity or dormancy of microorganisms in highly compacted bentonites as a result of severe environmental constraints (e.g., low water activity and high swelling pressure in the confined bentonite) *in situ* would be expected to largely inhibit bacterial activity in highly compacted clay-based barriers in a future DGR.

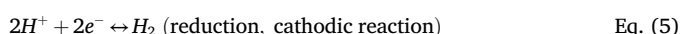
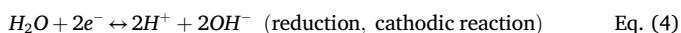
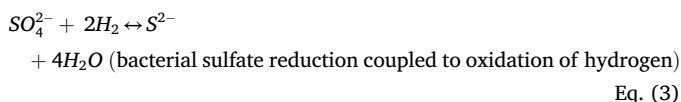
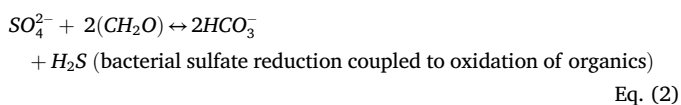
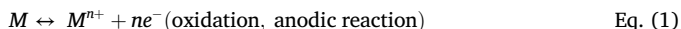
* Corresponding author.

E-mail address: darren.korber@usask.ca (D.R. Korber).

1. Introduction

Since the development of plans to dispose of spent nuclear fuel (SNF) in corrosion-resistant canisters within deep underground repository (DGR) facilities, the interest of engineers and scientists in bentonite clay materials as components of highly compacted engineered barriers has increased significantly. This is due to the remarkable ability of some types of bentonites to swell in the presence of water, thereby sealing all the cavities between the SNF canisters and host rocks, resulting in the isolation of the emplaced SNF from the environment. For the highly compacted bentonite clay that will be used in DGRs, space will be very confined, which will severely limit the swelling, resulting in a significant pressure increase, an effect that will limit both access to water and physical space for microorganisms to grow. To ensure the long-term isolation of this hazardous nuclear material, regulatory processes governing the construction and operation of DGRs have required in-depth analysis of various factors that may compromise the performance of barrier materials. Control of undesirable microbial activity in the close vicinity of SNF containers, e.g., within the highly compacted bentonite, is among a number of risks that need to be examined. Microorganisms are distributed ubiquitously throughout both natural and anthropogenic environments, including DGR settings. While most metabolically-diverse microbial species present in a DGR pose low risk to the integrity of barrier systems, the activity of certain organisms can lead to corrosive effects on metal canisters.

Modern designs of containers for SNF and other highly-radioactive waste forms rely on different metallic materials (i.e., copper and iron alloys) that are susceptible to corrosion reactions (King, 2013). Corrosion is the net electrochemical surface process resulting in metal oxidation and release of metal ions. Under anoxic conditions, which will prevail within a future DGR throughout most of its lifecycle, microbial activity is a critical parameter with the potential to accelerate the corrosion of metal containers (King, 2009). Being both active electrochemical agents and natural catalysts, bacteria have been hypothesised to take up electrons directly from metal surfaces (e.g., iron), thereby oxidizing metals (Eq. 1) or by deteriorating them indirectly through excretion of bacterial metabolites that corrode materials (Dinh et al., 2004). For instance, sulfide, produced due to bacterial reduction of sulfate (Eq. 2), is a key biogenic product which facilitates anodic and cathodic corrosion reactions (Enning and Garrelfs, 2014). Hydrogenotrophic prokaryotes scavenge molecular hydrogen (Eq. 3) liberated in cathodic reactions (Eqs. (4) and (5)) permitting the sustained passage of metal ions into solution, leading to corrosion of the metal. Dissolved biogenic sulfide ions react with metals (Eqs. (6) and (7)) resulting in poorly-soluble metal-sulfide products that, under appropriate conditions, either passivate or corrode metal surfaces (Enning and Garrelfs, 2014). In general, microbial acid production results in the removal of protective oxide layers from metal interfaces, followed by anodic dissolution of the metal along with the cathodic reduction of water and protons (Eqs. (4) and (5)).



Testing of microbiologically-accelerated corrosion requires a combination of microbiological, chemical and physical methods. Microbiological tools are used to confirm the biological nature of corrosion phenomena, while physical and chemical techniques inspect spatio-temporal effects of the microbial activity on the material integrity. Traditionally, microbiologists have relied on enrichment-based procedures (e.g., colorimetric or precipitate formation) to confirm the presence or absence of acid- and sulfide-producers. This approach is tedious and only reveals a minor fraction of an existing microbial population. Contemporary molecular and biochemical techniques that examine biological markers (e.g., nucleic acids, phospholipid-derived fatty acids, etc.) in environmental samples are faster, more reliable, and specific (Spiegelman et al., 2005). Comparative analysis of specific genetic markers (e.g., 16S rRNA genes) permits the identification of the microbial species present, as well as the extrapolation of that taxonomic diversity to the metabolic inventories of the bacteria discovered that enables them to deteriorate industrial materials, such as metals (Abhauer et al., 2015; Bomberg et al., 2016; Jun et al., 2015; Langille et al., 2013; Rajala et al., 2017). Because the ecological function of a microbial community is the result of complex trophic interactions between various bacteria with different physiological capabilities, it is reasonable that to delineate metabolic functions of concern to a DGR, the focus should be on those biochemical reactions that directly or indirectly contribute to the corrosion of metals.

Cell mechanisms that enable bacteria to accept electrons directly from metal surfaces remain largely unexplored (Deng et al., 2018; Enning and Garrelfs, 2014). However, recent findings from novel genomic and gene expression technologies for profiling bacterial populations associated with bioelectrochemical systems (e.g., corrosion sites and microbial fuel cells) have revealed useful information about potential enzymatic machinery active in other corrosion-like reactions (i.e., as reviewed in Blasco-Gómez et al. (2017), Chong et al. (2018), Kouzuma et al. (2018) and Kryachko and Hemmingsen (2017)).

Microbial reduction of molecular hydrogen and protons on metal surfaces is catalyzed by reversible hydrogenases (Bryant et al., 1991; Bryant and Laishley, 1990; de Silva Muñoz et al., 2007; Mehanna et al., 2008; Silva et al., 2002). Similar enzymes likely participate in direct electron transfer with the steel surface (Mehanna et al., 2009). Extracellular surface-associated hydrogenases have been shown capable of mediating apparent electron uptake leading to the liberation of hydrogen gas (Deutzmann et al., 2015). Furthermore, there is a line of evidence to suggest that extracellular formate dehydrogenases are also capable of liberating electrons from cathodic surfaces and catalyzing the production of formate (Deutzmann et al., 2015).

Besides the function of reversible hydrogenases, processes most detrimental to metal stability involve dissolved sulfide resulting from microbial reduction of various sulfur oxyanions (e.g., sulfate, thiosulfate) as well as from disproportionation of elemental sulfur. The dissimilatory reduction of sulfate to sulfide proceeds via activation of sulfate with ATP by the enzyme sulfate adenylyltransferase (Sat), producing adenosine phosphosulfate (APS). Adenosine phosphosulfate is reduced subsequently to bisulfite by APS reductase (AprBA), which is reduced to sulfide by dissimilatory sulfite reductase (DsrAB) (Rabus et al., 2015). In addition to metabolizing sulfate and bisulfite, most sulfate-reducing microorganisms can also use thiosulfate as an electron acceptor via the enzyme thiosulfate-reductase (PhsABC) that reduces thiosulfate to bisulfite, which is metabolized further to sulfide by DsrAB (Rabus et al., 2015). Another microbial mechanism of sulfide production involves the disproportionation of thiosulfate, sulfite or elemental sulfur with sulfate as an additional end-product (Rabus et al., 2015).

Corrosive effects of microbial activity are more complex than just depolarisation of metal surfaces or production of sulfide. Bacteria are

capable of producing a number of weak acids (e.g., carbonic and acetic acids) that are generally considered to be key factors, along with sulfide in hydrogen embrittlement of metals, leading to increased corrosion rates (Pope et al., 1988). Bacteria produce acids and carbon dioxide from fermentation and decomposition of organic matter (Kryachko and Hemmingsen, 2017). However, fermentable substrates are not expected to occur widely in engineered barrier systems; therefore, microorganisms will likely rely on the fixation of mineral carbon (e.g., HCO_3^- , CO_3^{2-} , CO_2) for growth in clayish systems (Bagnoud et al., 2016; Grigoryan et al., 2018). Some bacteria (e.g., acetogenic bacteria or acetogens) are capable of reducing CO_2 to acetate for the production of energy, as well as of fixation of CO_2 for cellular carbon (Drake et al., 2013). These obligate anaerobes employ the reductive acetyl-CoA pathway for the synthesis of the acetyl moiety of acetyl-CoA from CO_2 (Drake et al., 2013).

In this report, we used a predictive approach to examine the taxonomic and functional diversity of bacteria in commercial clays, some of which (e.g., MX-80) are similar to those specified in the Canadian DGR design, to obtain a better understanding of how resident microorganisms could potentially contribute to the bio-deterioration of metal constituents of a clay-based engineered barrier system.

2. Material and methods

2.1. Source of clays

Clay materials utilized in this study included: 1) two different lots of Volclay MX-80® clay (American Colloid Company) purchased at different times, and hereafter referred to as MX-80 Batch 1 and MX-80 Batch 2, respectively, and 2) Canaprill® (Canadian Clay Product Inc.). Presently, MX-80 bentonite is the reference engineered barrier material for the Canadian DGR concept (Villagran et al., 2011). The MX-80 Batch 2 sample is similar to the clay material to be used in the Material Corrosion Test (MaCoTe; <http://www.grimsel.com/gts-phase-vi/macote-the-material-corrosion-test/macote-introduction>, link accessed on May, 2021) at the Grimsel test site (Switzerland). Background data and elemental composition of MX-80 and Canaprill bentonites have been reported elsewhere (Grigoryan et al., 2018).

2.2. Media, cultivation conditions and sulfide assays

Indigenous clay microorganisms were enriched in replicate (MX-80 Batch 1 and Canaprill samples were incubated in four replicates, MX-80 Batch 2 – in duplicate) anoxic microcosms composed of 10% w/v bentonite in modified Zeikus's medium (Zeikus et al., 1975): NH_4Cl (0.9 g/L), NaCl (0.9 g/L), $\text{MgCl}_2 \cdot 6\text{H}_2\text{O}$ (0.2 g/L), KH_2PO_4 (0.75 g/L), K_2HPO_4 (1.5 g/L) and 0.15 mL/L of 1% (w/v) resazurin. The medium was pre-reduced using a dispensing system (Glasgerätebau Ochs GmbH, Germany), autoclaved, and then cooled under a 80% (v/v) N_2 , 10% (v/v) H_2 , 10% (v/v) CO_2 atmosphere as described by Widdel and Bak (1992). Prior to dispensing, NaHCO_3 (2.5 g/L), FeSO_4 (15 mg/L), microelements (Pfennig and Lippert, 1966), selenate/tungstate (Widdel and Bak, 1992) and $\text{Na}_2\text{S} \cdot 9\text{H}_2\text{O}$ (250 mg/L) were added from sterile anoxic stock solutions and the pH adjusted to 7.4. Microcosms were prepared by mixing of sterile anoxic media (45 ml) with 5 g non-sterile clay material (see above) in pre-autoclaved 160 ml borosilicate glass bottles. After the clay-media slurries were flushed continuously for 2–3 min with the aforementioned gas mixture, the bottles were closed tightly with sterilized butyl rubber stoppers and crimped with aluminum rings. Thereafter, microcosms were transferred to a Forma anaerobic chamber model 1025/1029 (ThermoFisher Scientific, Marietta, OH) and a sterile 18 G x 1 1/2 in. PrecisionGlide needle (BD Biosciences, San Jose, CA, USA) attached to a 0.2- μm pore-size nitrocellulose filter (Millipore, Billerica, MA) was inserted through the rubber stoppers for periodic circulation of the H_2 -containing gas mixture above the clay suspensions. Accordingly, the H_2 -containing gas

mixture inside the bottles was replenished manually each day using a single evacuation-injection cycle via syringe in the anaerobic chamber, and then shaken briefly. Otherwise, the microcosms were kept stationary during incubation inside the anaerobic chamber at room temperature (RT) for eight and a half months (e.g., 260 days), unless otherwise indicated. While in the anaerobic chamber, 0.5 ml aliquots of clay suspensions were subsampled aseptically and concentrations of aqueous sulfide in microcosms were assayed photocolometrically using N,N-dimethyl-p-phenylenediamine sulfate reagent (Grigoryan et al., 2018; Trüper and Schlegel, 1964).

Microcosms containing autoclaved clays (with duplicates of each of the 3 types of clay) were used as abiotic controls and were assembled and handled the same as non-sterile treatment microcosms described above. Incubations with *as-received* clays in the Zeikus's medium under 100% (v/v) N_2 were set up additionally as no H_2 controls (data not shown).

2.3. DNA extraction and 16S rRNA amplicon sequencing

After 120 days of incubation the genomic DNA from the clay microcosms was extracted using the FastDNA SPIN kit for soil (MP Biomedicals Inc., Carlsbad, CA) according to the manufacturer's recommendations. Cell lysis was performed by bead beating of 0.5 ml clay suspension using the Precellys24 homogenizer (Bertin Technologies, Paris, France) at 6000 rpm for three 40 s-cycles. Amplicon libraries were prepared by PCR amplification of the V3–V4 regions of the bacterial 16S rRNA gene using the primers Bakt_341F and Bakt_805R (Herlemann et al., 2011) with Illumina overhang adaptors attached to their 5' ends. Conditions of the initial PCR amplification of 16S rRNA gene fragments, index-PCR using Nextera XT adapters (Illumina, Inc., San Diego, CA), amplicon purification, visualization and quantification steps have been described elsewhere (Grigoryan et al., 2018). Further normalization and processing of attained libraries was performed according to the Illumina guide (Part # 15044223 Rev. B). Aliquots containing 6 pM pooled DNA libraries were loaded onto a MiSeq Reagent Kit V3 cartridge (600 cycles) and sequenced on a MiSeq System (Illumina, Inc., San Diego, CA) in accordance with the manufacturer's instructions.

2.4. Processing of Illumina bacterial 16S rDNA libraries

The paired-end MiSeq reads (2 × 300 bp) from the three microcosm samples were assembled and transformed to contigs using FLASH code (Magoč and Salzberg, 2011), resulting in a total of 2528467 reads. Quality metrics of the datasets was controlled by FastQC code version 0.11.5 (<https://www.bioinformatics.babraham.ac.uk/projects/fastqc/>, link accessed on August 12, 2018). The yielded reads were assigned to their respective samples and clustered into operational taxonomic units (OTUs) using Quantitative Insights into Microbial Ecology (QIIME) package version 1.9.1 (Caporaso et al., 2010) according to the closed reference protocol based on Greengenes database version 13.8 (McDonald et al., 2012) with reference sequences congregated with a 97% similarity cut-off. To predict the metabolic repertoires of the different bacterial populations in the tested clays, the 16S rRNA gene libraries were processed through PICRUSt (Phylogenetic Investigation of Communities by Reconstruction of Unobserved States) version 1.1.0 code, a program that predicts functional profiles of microbial communities using 16S rDNA sequences and available databases of reference genomes (Langille et al., 2013). Using 16S rRNA genes as taxonomic and phylogenetic indicators, PICRUSt integrates frequencies of occurrence of specific 16S rRNA gene fragments in sequenced libraries with the 16S rRNA copy number for each taxon in a 16S rRNA-based microbial phylogeny and predicts the abundances of specific bacteria within the complex microbial population. The functional profile of the entire microbial population was derived based on information from available genome annotation databases (i.e., Integrated Microbial Genomes and Microbiomes system [Markowitz et al., 2012]) about metabolic capabilities of taxa contributing to microbial communities and retrieval of 16S rRNA

copy number information and metabolic footnotes from the Kyoto Encyclopedia of Genes and Genomes Orthology (Kanehisa et al., 2012). In the current study, PICRUSt was implemented to predict the occurrence of bacteria that harboured enzymes participating either in dissimilatory sulfate reduction, the Wood–Ljungdahl pathway of acetate production and the pool of hydrogenases for H₂ uptake in the different clay microcosms. Table 1 outlines the enzymes that were queried by PICRUSt in the form of KEGG Orthology (KO).

2.5. Statistical analysis

Percent values of putative contributions of each OTU (assigned at the family level) to a particular gene function per each of three reconstructed microbiomes of clay microcosms (i.e., MX-80 Batch 1, MX-80 Batch 2,

and Canapril) were retrieved from PICRUSt and correlated with the occurrence of the involved OTUs. Using OriginPro 2016 software (Origin Labs, Northampton, MA), the datasets obtained were ranked using the Kruskal–Wallis test based on frequencies of an OTU per sample and on the assumed contribution of the OTU in different gene pools. The taxon ranks per clay microcosms were converted further into percentages using the total number of contributing family-level OTUs. Finally, the potential inputs of the specific bacterial families contributing most-frequently to a particular metabolic function were summarized in bar charts using OriginPro 2016 software.

Potential corrosion threats in each sample were proxied by normalized frequencies of OTUs (AbundanceInSample) that were projected by the PICRUSt's script predict_metagenomes.py to harbour potentially-corrosive enzymatic pathways (e.g., sulfide production, acetogenesis

Table 1. Overview of KEGG orthologies showing genes belonging to pathways predicted to exist by PICRUSt based on the 16S rRNA gene amplicon libraries retrieved from clay incubations.

KEGG Orthology	Gene/protein	Enzyme definition	Overall Reaction
1. Dissimilatory sulfate reduction			
K00395	aprB	adenylsulfate reductase, subunit A	sulfite + AMP + an oxidized electron acceptor + 2 H ⁺ ↔ adenosine 5'-phosphosulfate + a reduced electron acceptor
K00394	aprA	adenylsulfate reductase, subunit B	sulfite + AMP + an oxidized electron acceptor + 2 H ⁺ ↔ adenosine 5'-phosphosulfate + a reduced electron acceptor
K11180	dsrA	dissimilatory sulfite reductase alpha subunit	(1) hydrogen sulfide + a [DsrC protein]-disulfide + 2 acceptor + 3 H ₂ O ↔ sulfite + a [DsrC protein]-dithiol + 2 reduced acceptor + 2 H ⁺ (overall reaction); (2) a [DsrC protein]-S-sulfanyl-L-cysteine + 3 acceptor + 3 H ₂ O ↔ sulfite + a [DsrC protein]-disulfide + 3 reduced acceptor + 2 H ⁺ (overall reaction);
K11181	dsrB	dissimilatory sulfite reductase beta subunit	(1) hydrogen sulfide + a [DsrC protein]-disulfide + 2 acceptor + 3 H ₂ O ↔ sulfite + a [DsrC protein]-dithiol + 2 reduced acceptor + 2 H ⁺ (overall reaction); (2) a [DsrC protein]-S-sulfanyl-L-cysteine + 3 acceptor + 3 H ₂ O ↔ sulfite + a [DsrC protein]-disulfide + 3 reduced acceptor + 2 H ⁺ (overall reaction)
K00958	met3, sat	sulfate adenylyltransferase	ATP + sulfate ↔ diphosphate + adenylyl sulfate
K00957	cysD	sulfate adenylyltransferase subunit 2	(1) ATP + sulfate ↔ diphosphate + adenylyl sulfate; (2) (1) ATP + Selenate ↔ Diphosphate + Adenylylselenate
K00956	cysN	sulfate adenylyltransferase subunit 1	(1) ATP + sulfate ↔ diphosphate + adenylyl sulfate; (2) (1) ATP + Selenate ↔ Diphosphate + Adenylylselenate
2. Reductive acetyl-CoA pathway (Wood-Ljungdahl pathway)			
K00194	cdhD, acsD	acetyl-CoA decarbonylase/synthase complex subunit delta	a [methyl-Co(III) corrinoid Fe–S protein] + tetrahydroarsinapterin ↔ a [Co(I) corrinoid Fe–S protein] + 5-methyltetrahydroarsinapterin
K00197	cdhE, acsC	acetyl-CoA decarbonylase/synthase complex subunit gamma	a [methyl-Co(III) corrinoid Fe–S protein] + tetrahydroarsinapterin ↔ a [Co(I) corrinoid Fe–S protein] + 5-methyltetrahydroarsinapterin
K00198	cooS, acsA	carbon-monoxide dehydrogenase catalytic subunit	CO + H ₂ O + 2 oxidized ferredoxin ↔ CO ₂ + 2 reduced ferredoxin + 2 H ⁺
K00297	metF, MTHFR	methylenetetrahydrofolate reductase (NADPH)	5-methyltetrahydrofolate + NAD(P) ⁺ ↔ 5,10-methylenetetrahydrofolate + NAD(P)H + H ⁺
K01491	folD	methylenetetrahydrofolate dehydrogenase (NADP [−])/methylenetetrahydrofolate cyclohydrolase	5,10-methylenetetrahydrofolate + NADP [−] ↔ 5,10-methylenetetrahydrofolate + NADPH + H ⁺ ; 5,10-methylenetetrahydrofolate + H ₂ O ↔ 10-formyltetrahydrofolate
K01938	fhs	formate–tetrahydrofolate ligase	ATP + formate + tetrahydrofolate ↔ ADP + phosphate + 10-formyltetrahydrofolate
K05299	fdhA	formate dehydrogenase alpha subunit	formate + NADP [−] ↔ CO ₂ + NADPH
K14138	acsB	acetyl-CoA synthase	acetyl-CoA + a [Co(I) corrinoid Fe–S protein] ↔ CO + CoA + a [methyl-Co(III) corrinoid Fe–S protein]
K15022	fdhB	formate dehydrogenase beta subunit	formate + NADP [−] ↔ CO ₂ + NADPH
K15023	acsE	5-methyltetrahydrofolate corrinoid/iron sulfur protein methyltransferase	a [methyl-Co(III) corrinoid Fe–S protein] + tetrahydrofolate ↔ a [Co(I) corrinoid Fe–S protein] + 5-methyltetrahydrofolate
3. Hydrogenases participating in H₂ uptake			
K05927	hydA	quinone-reactive Ni/Fe-hydrogenase small subunit	H ₂ + menaquinone ↔ menaquinol
K05922	hydB	quinone-reactive Ni/Fe-hydrogenase large subunit	H ₂ + menaquinone ↔ menaquinol
K06282	hyaA, hybO	hydrogenase small subunit	H ₂ + acceptor ↔ reduced acceptor
K06281	hyaB, hybC	hydrogenase large subunit	H ₂ + acceptor ↔ reduced acceptor
K00436	hoxH	NAD-reducing hydrogenase large subunit	H ₂ + NAD ⁺ ↔ H ⁺ + NADH
K00437	hydB	[NiFe] hydrogenase large subunit	H ₂ + 2 ferricytochrome c3 ↔ 2 H ⁺ + 2 ferrocyclochrome c3
K00533	E1.12.7.2L	ferredoxin hydrogenase large subunit	H ₂ + 2 oxidized ferredoxin ↔ 2 reduced ferredoxin + 2 H ⁺
K00532	E1.12.7.2	ferredoxin hydrogenase	H ₂ + 2 oxidized ferredoxin ↔ 2 reduced ferredoxin + 2 H ⁺
K00534	E1.12.7.2S	ferredoxin hydrogenase small subunit	H ₂ + 2 oxidized ferredoxin ↔ 2 reduced ferredoxin + 2 H ⁺
K06441	E1.12.7.2G	ferredoxin hydrogenase gamma subunit	H ₂ + 2 oxidized ferredoxin ↔ 2 reduced ferredoxin + 2 H ⁺
K00441	frhB	coenzyme F420 hydrogenase subunit beta	H ₂ + oxidized coenzyme F420 ↔ reduced coenzyme F420

and hydrogen uptake) were extracted from the OTU table and multiplied by relative abundance of the KO family in the sample (Contribution PercentOfSample). The result was divided by the relevant number of assayed gene families. Furthermore, results for each family level taxon per each group of treat per sample were summed according to Eq. (8):

$$p(MC) = \sum \frac{A \times X}{l} + \sum \frac{B \times Y}{m} + \sum \frac{C \times Z}{n} \quad \text{Eq. (8)}$$

where:

A - normalized abundance of OTUs at the family level that potentially possess genes encoding hydrogenases contributing to hydrogen uptake,

B - normalized abundance of OTUs at the family level that potentially possess genes encoding enzymes of the Wood–Ljungdahl pathway,

C - normalized abundance of OTUs at the family level that potentially possess genes encoding enzymes contributing to sulfide production, X- relative abundance of the KO of hydrogenases of the hydrogen uptake in the sample, which is potentially carried by the specific OTUs, Y - relative abundance of the KO of the Wood–Ljungdahl pathway in the sample, which is potentially carried by the specific OTUs, Z - relative abundance of the KO of the sulfide production in the sample, which is potentially carried by the specific OTUs,

l - total number of assayed KO related to hydrogen uptake (viz. 11)

m - total number of assayed KO related to the Wood–Ljungdahl pathway (viz. 10)

n - total number of assayed KO related to sulfide production (viz. 7)

These total sums were subjected to PCA using OriginPro 2016 software and projected onto a 2D plane where the eigenvectors' disposition indicates the direction of maximum variance in the data associated with different clays; whereas, the length of the eigenvector reflects the extent of variance within examined groups of data. OTUs with high principal component scores were most abundant and/or possessed a larger number of corrosion-inducing capabilities (i.e., higher potential corrosion risk) and were consequently located further from the center of the PCA plot. Alternatively, the OTUs with the lowest abundances and/or incomplete functional pathways were located closer to the center of the PCA plot, and likely posed minimal corrosion threats.

2.6. Nucleotide sequence accession numbers

Illumina sequence data from this study have been deposited in the NCBI Sequence Read Archive under the project accession number PRJNA719485.

3. Results

3.1. Production of sulfide in clay microcosms supplemented with 10% hydrogen

Sustained production of sulfide in the hydrogen-fed microcosms with MX-80 Batch 1 was detected after 22 days of incubation at RT (Figure 1). As much as 3.9–4.2 mmole of sulfide was produced in tests with MX-80 Batch 1 after 250 days (data not shown). Sulfide accumulation was visually-indicated by the appearance of a conspicuous black layer at the clay-liquid interface, which subsequently spread into deeper layers of the clay matrix.

Incubation of Canaprill clays in the presence of 10% hydrogen resulted in transient production of 0.4–1.2 mmole of sulfide, which generally disappeared within 2–3 days (Figure 1). Small amounts of sulfide accumulation reoccurred after 5–14 days followed again by a lowering in measurable soluble sulfide. These short-term accumulations and losses of sulfide were accompanied by the blackening of clays when sulfide was present, followed by the pale pink coloration of resazurin in

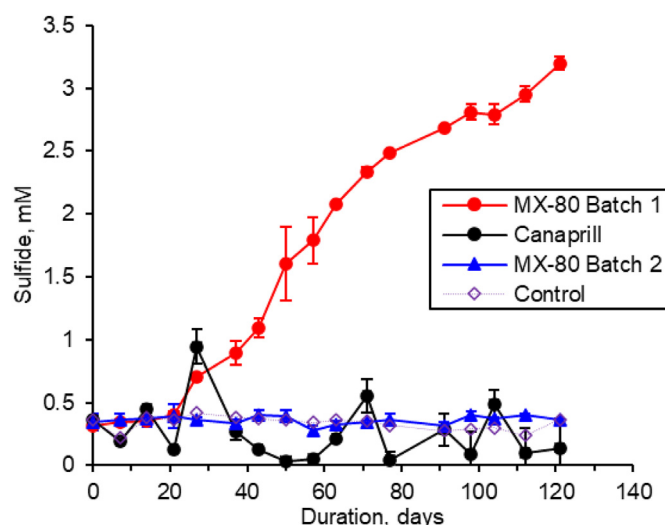


Figure 1. Production of sulfide in microcosms containing either MX-80 Batch 1 (■), Canaprill (●) and MX-80 Batch 2 (▲) clays under 10% H₂ atmosphere. Data represent averages of triplicate sulfide measurements collected during 121 days of incubation; error bars represent standard deviations. Control curve depicts the average total of duplicate sulfide measurements of autoclaved clay microcosms.

the medium and yellowing or blanching of the sediment in the absence of sulfide. This cyclic trend was observed in three of four replicate incubations over a six-month period, and in one of the bottles sulfidogenesis recovered after 75 days and generated approximately 1.8 mmol sulfide after 250 days of incubation (data not shown).

No sulfide production was detected in MX-80 Batch 2 microcosms after 90 days of incubation under 10% hydrogen atmosphere (Figure 1), although the medium consistently remained colourless and hence anoxic, a requirement for sustainable growth of sulfate-reducing bacteria.

Similarly, no generation of sulfide was found in control pre-autoclaved clay microcosms (Figure 1) and in clay enrichments with no exogenous hydrogen gas nor organics (data not shown).

3.2. Assessment of bacterial diversity in hydrogen-fed clay microcosms using 16S rRNA gene amplicons sequencing

High-throughput sequencing of bacterial 16S rRNA gene amplicons revealed that bacteria from H₂-stimulated clay microcosms were affiliated with at least 9 phylum-level groups. The contributions that members of different phyla made to the different clay bacterial communities varied (Figure 2A).

The dominant phylum in MX-80 Batch 1 libraries was Firmicutes (82%), with relatively smaller fractions of Chloroflexi (13.5%) and Proteobacteria (3.9%). Members of these three phyla made up over 99% of Batch 1 MX-80 16S rRNA gene sequencing libraries (normalized for the size of the individual libraries). The bacterial families *Clostridiaceae* (20%), *Peptococcaceae* (13.8%), *Peptostreptococcaceae* (33.7%) and *Bacillaceae* (4.4%) were predominant among identified Firmicutes from MX-80 Batch 1 (Figure 2A). Some other 16S rRNA gene sequences were also classified at the family level; however, they made up a relatively small portion of the MiSeq libraries (low abundance, <3%) and thus are not discussed further. In addition, Figure 2B outlines a relative abundance of certain bacterial 16S rRNA amplicons across H₂-fed clay microcosms that were classified at the genus-level.

The most abundant OTU's in amplicon libraries from Canaprill enrichments were affiliated with the phyla Proteobacteria (70.5%), with minor contributions from Firmicutes (15.6%), Acidobacteria (7.4%), Bacteroidetes (3.1%), and Actinobacteria (1.5%) (Figure 2A). Members of the bacterial families *Pseudomonadaceae* (30.4%), *Hydrogenophilaceae* (13.4%), *Desulfobacteraceae* (5.7%), *Desulfobulbaceae* (4.5%) were most

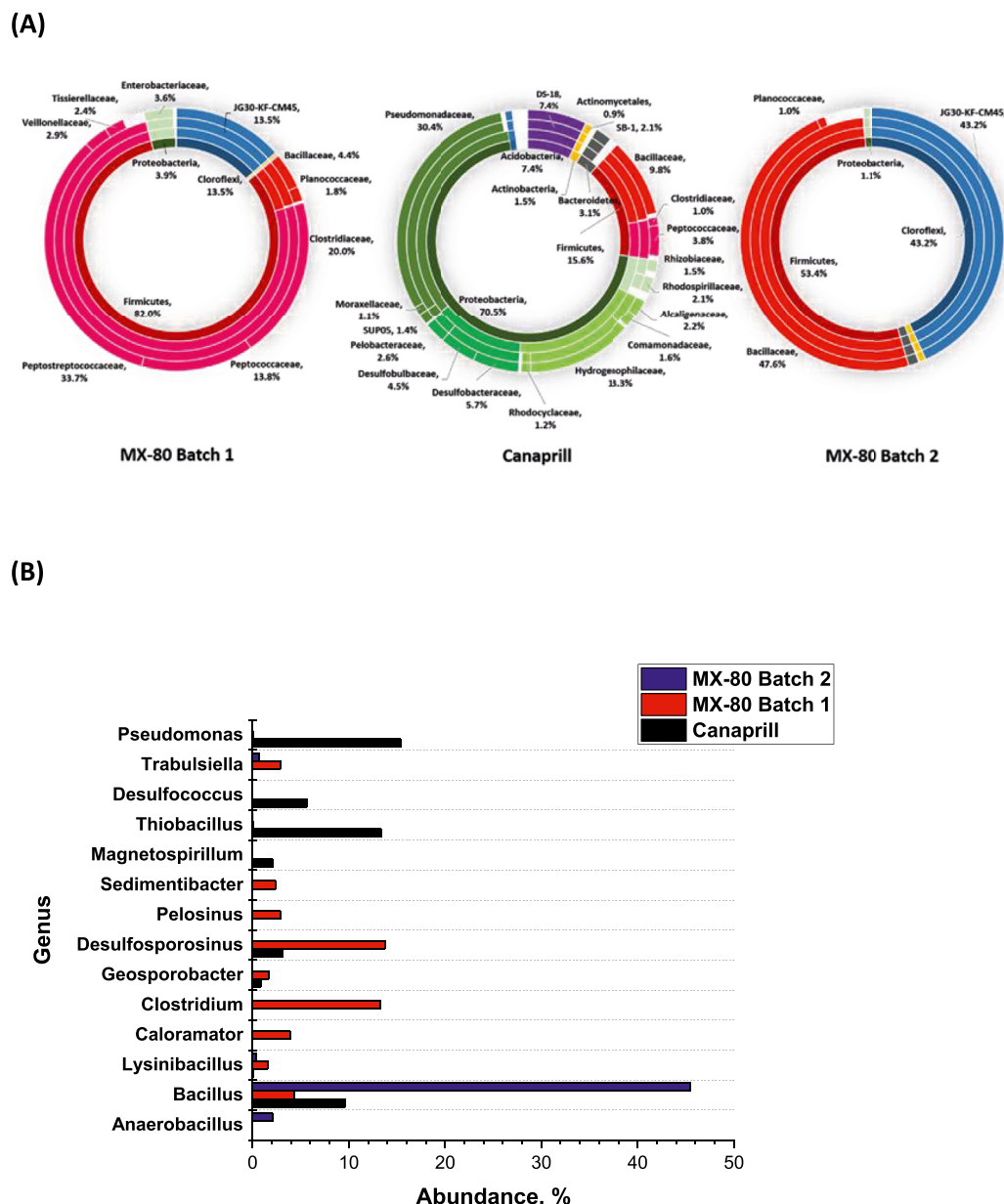


Figure 2. Diversity and relative abundance (>1%) of OTUs inferred from high-throughput sequencing of the bacterial 16S rRNA gene amplicon libraries from H₂-fed sulfate-rich clay microcosms. Panel (A) outlines the phylum- (inner segments) and family- (outer segments) level diversity. Unlabeled segments in the middle correspond to class and order level taxa. Panel (B) depicts the genus-level diversity in the above H₂-fed sequenced libraries.

abundant (>3%) among the phylum Proteobacteria, whereas *Bacillaceae* (9.8%) and *Peptococcaceae* (3.8%) were most abundant among members of the phylum Firmicutes.

Identified gene sequences from the MX-80 Batch 2 microcosms primarily belonged to the phylum Firmicutes (53.4%), along with Chloroflexi (43.2%) (Figure 2A). Firmicutes were mostly represented by bacteria of the family *Bacillaceae* (47.6%).

Chloroflexi sequences from all clay enrichments were affiliated with the order JG30-KF-CM45 of the class Thermomicrobia, except non-abundant sequences in Canapril enrichments that were assigned to the class Anaerolineae (Figure 2A).

3.3. PICRUSt-based prediction of specific metabolic features within hydrogen-stimulated bacterial populations in clay microcosms

From the 16S rRNA gene sequence libraries retrieved from the clay microcosms, PICRUSt identified 328 KEGG pathways. Removing non-

prokaryotic pathways as well as low relative abundance pathways (<1%) from the three data sets resulted in a total of 62 dominant pathways mostly related to cell maintenance (e.g., transporters, genetic information processing, environmental information processing, etc.) and metabolism (Figure 3). In addition, we compared the predicted presence (i.e., percentage relative abundance) of certain KEGG reference pathways of either high or low abundance (<1%) that could be associated potentially with corrosion risks within the clay microcosms (sulfur metabolism, carbon fixation and fatty acids metabolism).

Considering KEGG orthologies (KO) responsible for dissimilatory sulfate reduction (Table 1) within the sulfur metabolism KEGG module, it was found that the bacterial families *Peptococcaceae*, *Clostridiaceae*, *Veillonellaceae*, *Lachnospiraceae*, *Hydrogenophilaceae* and *Enterobacteriaceae* were most abundant in MX-80 Batch 1 microcosms within family-level taxa (Figure 4), harbouring a variable set of genes coding for enzymes involved in dissimilatory sulfate reduction (or in potential reverse reactions). However, only certain genera from the above list (i.e.,

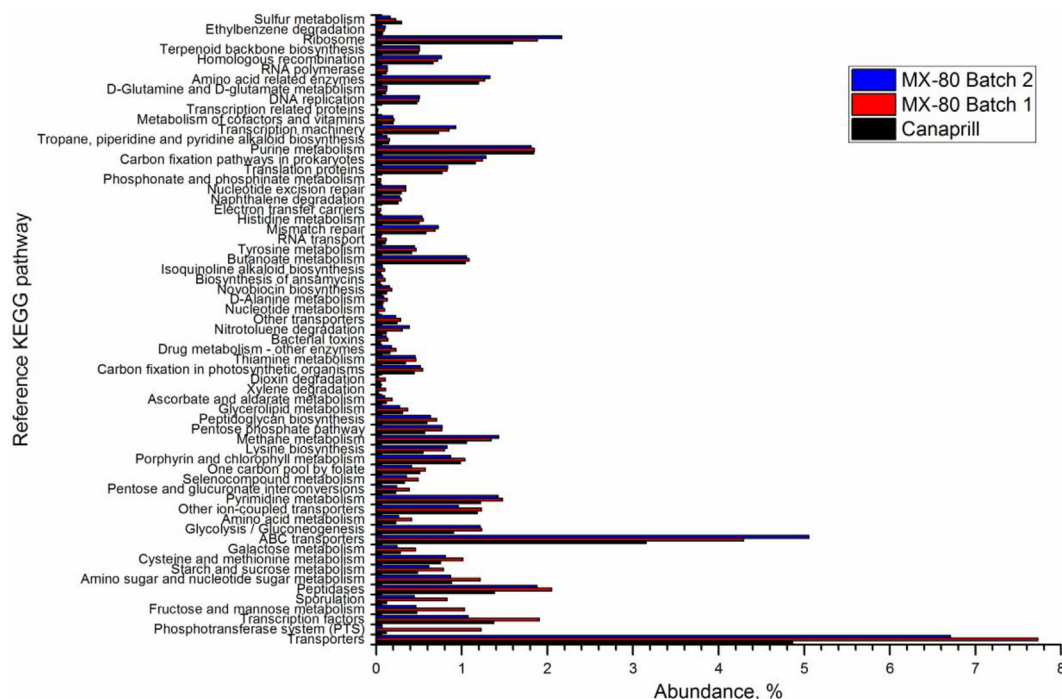


Figure 3. The relative abundance of the most variable KEGG pathways comprised of predicted genes retrieved via PICRUSt analysis from 16S rRNA libraries for bacterial populations in H₂-fed sulfate-rich clay microcosms.

Peptococcaceae, *Veillonellaceae*, *Hydrogenophilaceae* and *Dehalobacteriaceae*) detected in MX-80 Batch 1 microcosms potentially host *aprA*, *dsrA* and *dsrB* genes that encode key enzymes for dissimilatory sulfate reduction and sulfur oxidation (Table 1). Detected members *Peptococcaceae* and *Hydrogenophilaceae* additionally possess *aprB*, a marker gene for active sulfur transformation, potentially making these bacteria leading contributors to corrosion processes linked to bacterial sulfur cycling in the microcosms containing MX-80 Batch 1 bentonite. Actually, the high ranks of families *Peptococcaceae*, *Veillonellaceae*, *Hydrogenophilaceae* and *Dehalobacteriaceae* shown in Figure 4 indicate that detected amplicons associated with these taxa were relatively abundant in the 16S rDNA libraries from MX-80 Batch 1 microcosms in comparison with other family-level taxa carrying genes of sulfur metabolism and presumably harbour the majority of genes encoding the dissimilatory sulfate reduction pathway, as detailed in Table 1.

The number of families that potentially possessed sulfur metabolism genes in Canaprill clay was greater than in the other clays, but occurred at lower frequencies (Figures 2 and 4). The core potential contributors to the pool of genes responsible for sulfur metabolism in Canaprill clay included the families *Comamonadaceae*, *Hydrogenophilaceae*, *Desulfobacteraceae*, *Desulfobulbaceae* and *Peptococcaceae*, but the members of *Hydrogenophilaceae* (13.3%), *Desulfobacteraceae* (5.7%), *Desulfobulbaceae* (4.5%) and *Peptococcaceae* (3.8%) were most abundant within these taxa harbouring *aprA*, *dsrA* and *dsrB* genes (Figures 2 and 4).

In the MX-80 Batch 2 microcosms, the bacterial 16S rRNA gene sequences possessing sulfur metabolism (Figures 2 and 4) were represented mainly by members of the families *Bacillaceae*, *Planococcaceae*, and *Celulomonadaceae*; however, none of detected taxa were known to have *aprA*, *dsrA* and *dsrB* genes. Notably, the only members of *Hydrogenophilaceae* within MX-80 Batch 2 enrichments found to carry sulfur reducing genes represented only 0.04% of the MX-80 Batch 2's clay 16S rRNA gene library.

As seen in Figure 3, the carbon fixation pathway was predicted in all clay microcosms to the same extent; however, the genes for Wood–Ljungdahl pathway of acetogenesis were found only in certain taxa and in these taxa, with few exceptions, the pathway was often incomplete (i.e., predicted taxa are known to harbour genes that code only a part of

enzymes contributing to the Wood–Ljungdahl pathway). For instance, in MX-80 Batch 1 microcosms members of family *Peptococcaceae*, whose sequences were abundant (13.8% of all detected sequences) in the 16S rRNA gene sequencing library from MX-80 Batch 1 enrichments, harboured almost a full set of genes required for acetogenesis, excluding the formate dehydrogenase beta subunit (*fdhB*). Certain members of two other predominant families, *Clostridiaceae* and *Peptostreptococcaceae* (occurring at 20 and 33.7% relative abundance, respectively), are also known to contain almost a full complement of genes needed to proceed with carbon fixation to acetate. Similarly, Canaprill sequences assigned to *Peptococcaceae* (3.8%) likely contributed to acetate production, even though they were less-abundant than in the MX-80 Batch 1 microcosms. Other prospective contributors to acetate production in the Canaprill microcosms were *Desulfobacteraceae* (5.6%) and *Pelobacteraceae* (2.6%) and some others (Figures 3 and 5). The representation of genes linked to acetogenesis within taxa assigned to very small fractions of the 16S rRNA library from hydrogen-fed MX-80 Batch 2 enrichments was limited. Key genes such as *fdhB* were likely associated with family *Deferribacteraceae*, while *cdhD* – with the order JG30-KF-CM45, a branch within the phylum Chloroflexi, was detected in the MX-80 Batch 2 16S rRNA gene sequencing libraries.

According to the PICRUSt analysis, nine of eleven examined KO (Table 1) relating to hydrogen uptake (Figure 6) were potentially present in MX-80 Batch 1 microcosms within members of 19 bacterial families, from which *Peptostreptococcaceae* (33.7%), *Clostridiaceae* (20%), *Peptococcaceae* (13.8%), *Bacillaceae* (4.4%), *Enterobacteriaceae* (3.6%) and *Veillonellaceae* (2.9%) were most abundant. K06281 and K06282 orthologies that corresponded to an ambiguous group of hydrogenases containing iron-sulfur (sometimes nickel-iron) clusters represented the most often-found hydrogenase-related KOs, identified in 12 out of 19 bacterial families occurring in MX-80 Batch 1 microcosms. Some families carried only that type of hydrogenase-related KO, and they were associated with [FeS] hydrogenases. Orthologs K00436 and K00433 (Table 1) were other often-observed groups of hydrogenases, seen in five and four out of 19 bacterial families, respectively, that were detected in MX-80 Batch 1 microcosms (Figure 6). Members of the families *Clostridiaceae*, *Peptococcaceae* and *Veillonellaceae* have been shown to carry

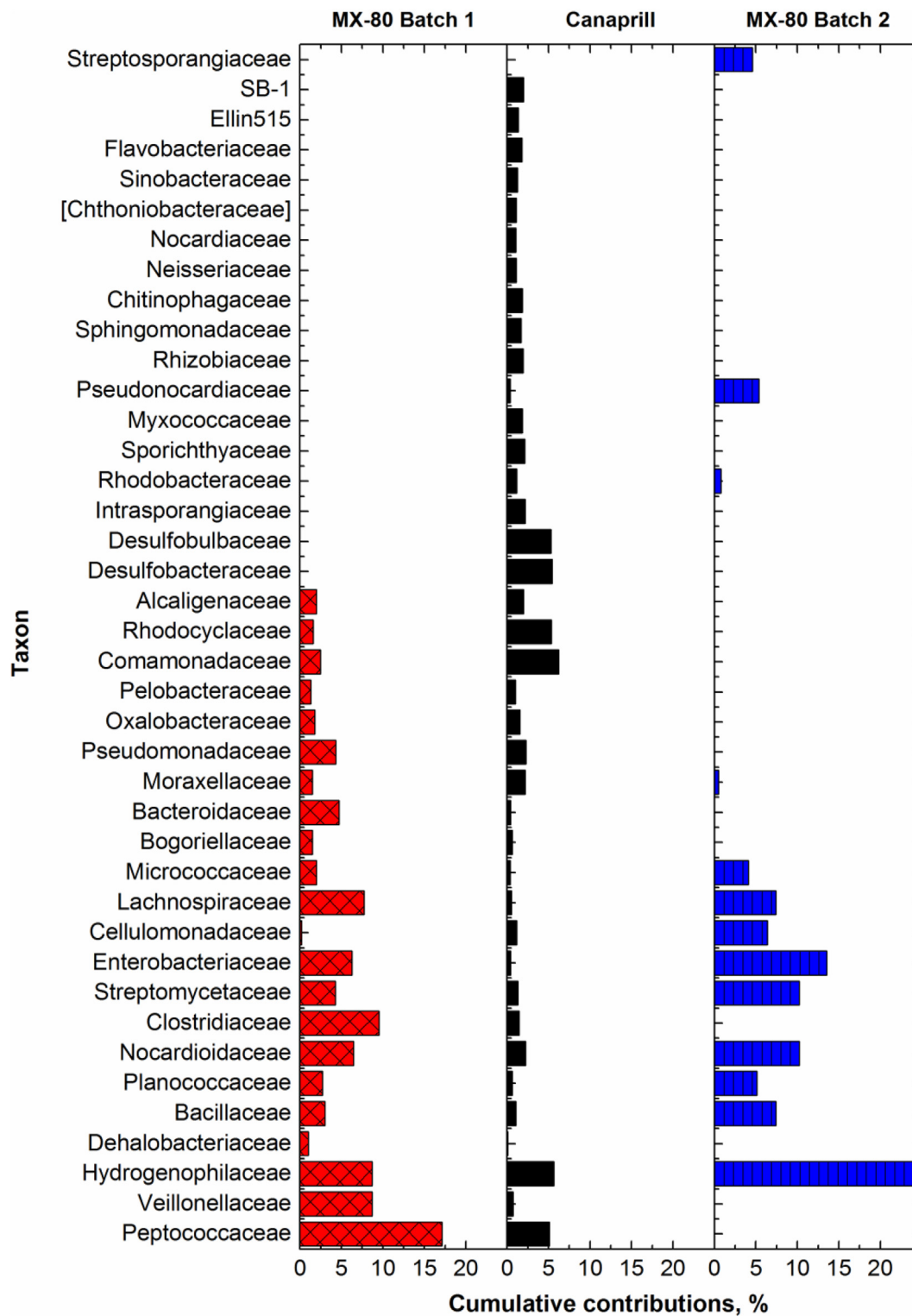


Figure 4. Cumulative putative contributions (%) of bacterial families to dissimilatory sulfate reduction pathways in H₂-fed clay microcosms.

different combinations of K00532, K00533 and K00437, in addition to K06281/K06282 (Table 1), making members of these families physiologically-versatile and potentially corrosively-active (Figure 6). Some other detected families (e.g., *Comamonadaceae* and *Rhodospirillaceae*) could potentially carry a large set of hydrogenases, though their sequences were scarce (<0.01%) in the Batch 1 MX-80 16S rRNA gene library; thus, they were likely not significant to the functioning of the entire community under the imposed conditions. In Batch 2 MX-80

microcosms the genes encoding H₂-scavenging enzymes were potentially present in families *Rhodobacteraceae*, *Enterobacteriaceae*, *Streptomycetaceae*, and some others that collectively make only 0.5% of the sequenced library.

Within members of 43 pathway families detected in Canapriil microcosms, the most often-observed orthologies were K06281, K00436, K06282 and K00441 (Table 1), predicted to occur in 24, 15, 13 and 10 different families, respectively (Figure 6). From pools of the most

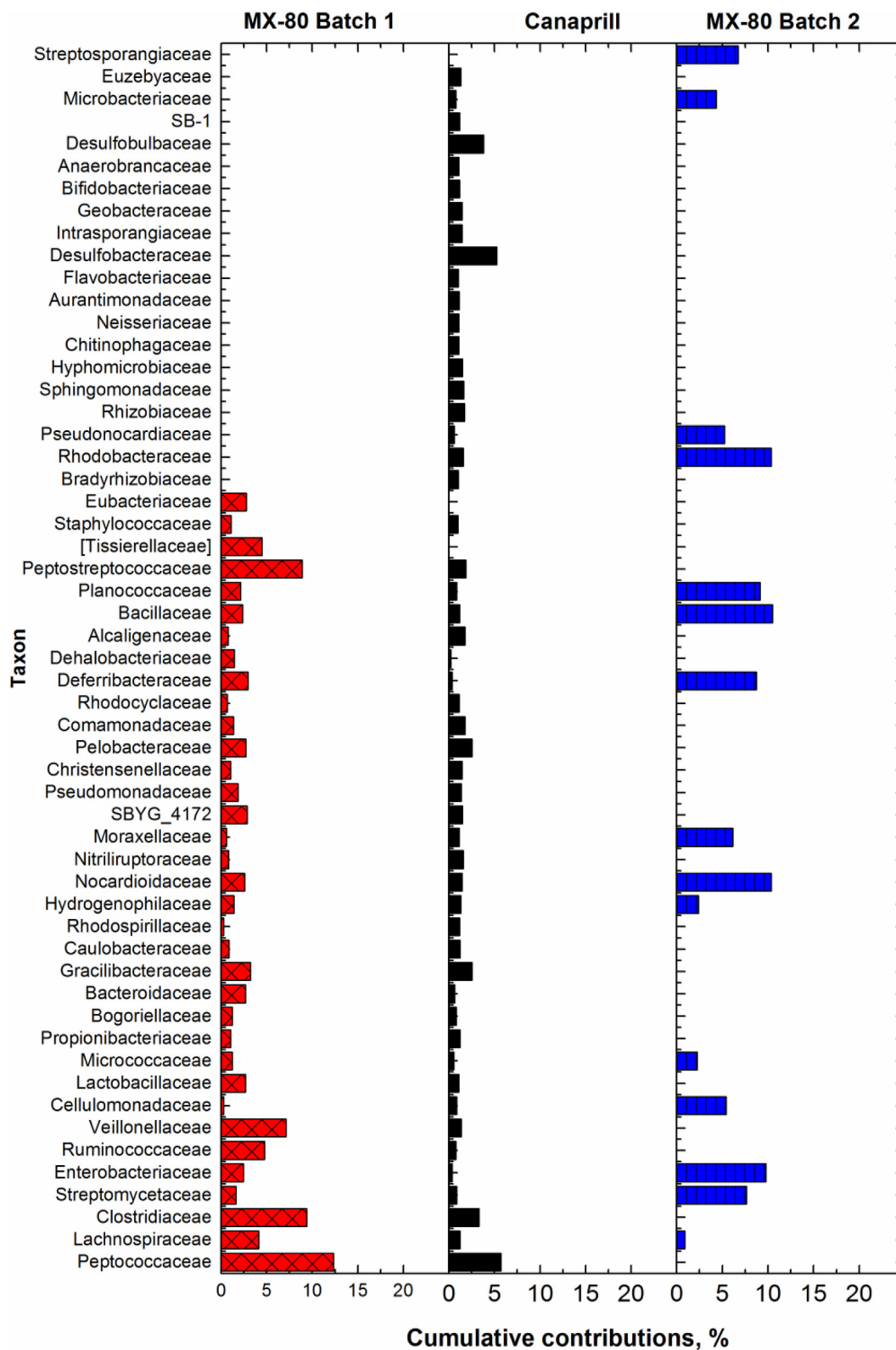


Figure 5. Cumulative putative contributions (%) of bacterial families to the Wood-Ljungdahl pathway in H₂-fed clay microcosms.

abundant (>1%) members of families *Hydrogenophilaceae* (13.3%), *Bacillaceae* (9.8%), *Desulfobacteraceae* (5.7%), *Desulfobulbaceae* (4.5%), *Peptococcaceae* (3.8%), *Alcaligenaceae* (2.2%), *Rhodospirillaceae* (2%), *Comamonadaceae* (1.6%), *Rhodocyclaceae* (1.2%) and *Clostridiaceae* (1%) [see Figure 2A], orthologies K06281 and K06282 were most-predicted in 7 families out of the 11 most-abundant families (members of family

Desulfuromonadaceae were projected to lack that KO), along with other less-often predicted KOs, i.e. K00441, K00437, K00436, K00532, K00534 and K06441 (Table 1). Detected bacteria of families *Peptococcaceae*, *Comamonadaceae*, *Rhodocyclaceae* and *Clostridiaceae* are known to carry several different hydrogen-uptake systems (i.e., either K06282/K06281, K00532, K00534, K00436/K00437 and/or K00441). Orthologies

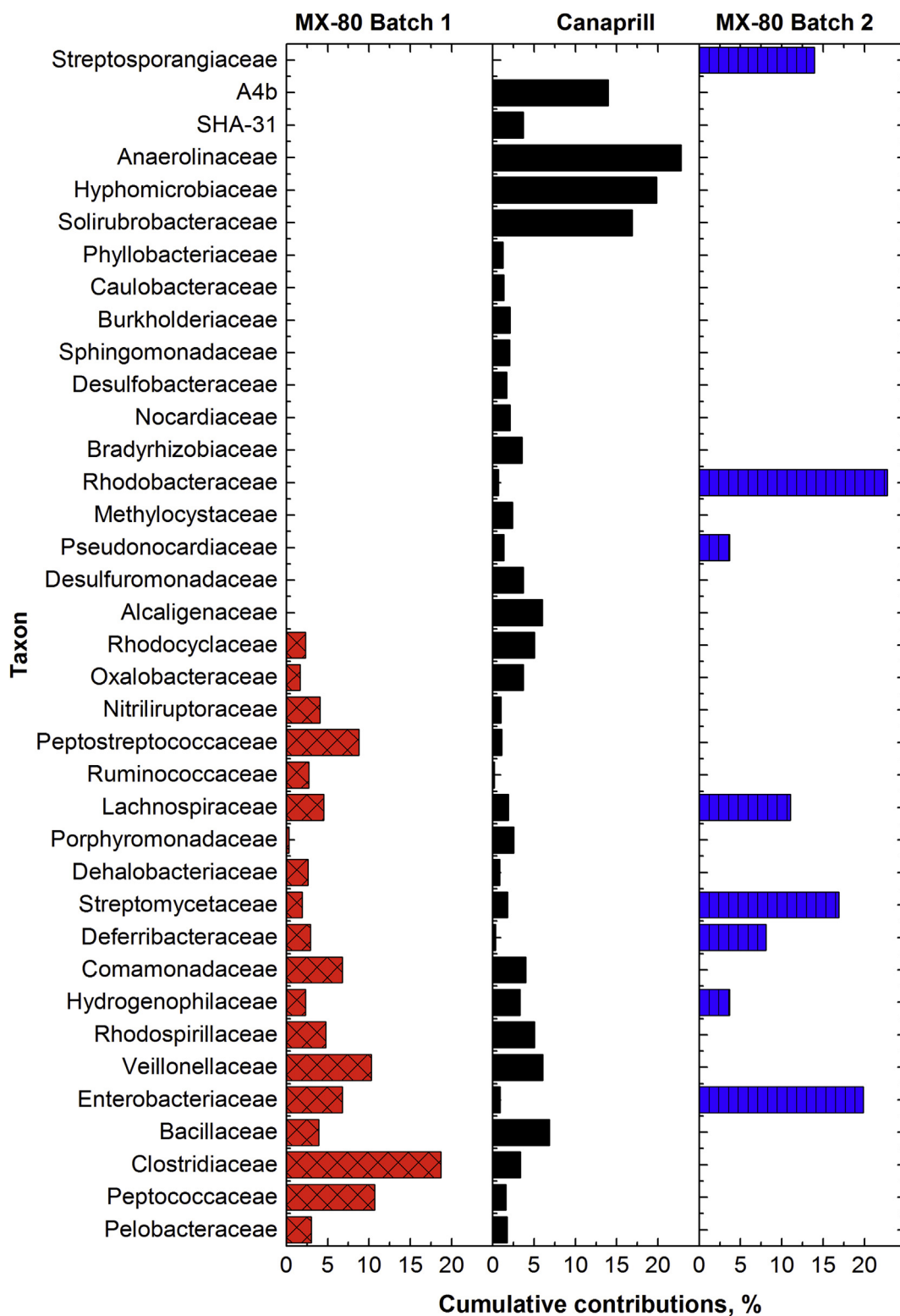


Figure 6. Cumulative putative contributions (%) of bacterial families to initial hydrogen uptake in H₂-fed clay microcosms.

K05922, K05927 and K00533 were less broadly distributed as they were predicted to occur only within low-abundance families.

Further reconciliation of sums of frequencies of genes-of-interest with taxonomic abundances in predicted metagenomes revealed that bacteria of families *Peptococcaceae*, *Clostridiaceae*, *Peptostreptococcaceae*, *Enterobacteriaceae*, *Hydrogenophilaceae*, *Bacillaceae*, *Pelobacteraceae*, *Pseudomonadaceae*, *Desulfobacteraceae* and *Desulfobulbaceae* were well-populated

and possessed versatile elements of metabolic pathways contributing to corrosive reactions in the examined clay enrichments. The PCA biplot shown in Figure 7 shows well-separated clay samples and related bacterial families, projecting the most prevalent and metabolically versatile taxa the furthest from the center of the plot. Thus, among these ten families, bacteria of *Peptostreptococcaceae*, *Hydrogenophilaceae* and *Bacillaceae* were found to be relatively most-abundant in MX-80 Batch 1,

Canapriil and MX-80 Batch 2 microcosms, respectively (Figure 7). Therefore, representatives of these families were assumed to pose higher corrosion risks than other bacteria detected in these microcosms. Bacteria of families *Peptococcaceae*, *Clostridiaceae* and *Enterobacteriaceae* were also considered to present a risk in MX-80 Batch 1 microcosms, but to a lesser degree than for *Peptostreptococcaceae* spp. (Figure 7). Similarly, *Peptococcaceae*, *Desulfobacteraceae*, *Desulfobulbaceae*, *Pelobacteraceae* and *Pseudomonadaceae* represented some corrosion threat, but smaller than bacteria of family *Hydrogenophilaceae*, in Canapriil microcosms (Figure 7). Similarly, bacteria of families *Hydrogenophilaceae* and *Enterobacteriaceae* were identified to pose some corrosion threats in MX-80 Batch 2 microcosms.

4. Discussion

Dissimilar patterns of sulfidogenesis in the tested clay microcosms under 10% hydrogen (Figure 1) were found to occur during long-term incubations. Accumulation of sulfide in MX-80 Batch 1 incubations were likely linked to growth of predominant, sulfate-reducing *Desulfo-*sporosinus** spp. of the family *Peptococcaceae* of the phylum Firmicutes. These bacteria are capable of reducing SO_4^{2-} (as well as SO_3^{2-} , $\text{S}_2\text{O}_3^{2-}$) to sulfide, coupled with the oxidation of hydrogen. In contrast, the sporadic production of sulfide in Canapriil microcosms could possibly be due to the activity of SRB of the proteobacterial families *Desulfobulbaceae* (4.5%) and *Desulfobacteraceae* (5.7%), as well as less-abundant Firmicutes of the family *Peptococcaceae*. Formed sulfide possibly could then undergo oxidation by Thiobacilli-like bacteria of the family *Hydrogenophilaceae*. This could explain the transient lowering of sulfide concentration with time in Canapriil enrichments; however, the nature of the electron acceptor used in this oxidative process under the imposed anoxic conditions remains unclear. Details on sulfur oxidative reactions in clay microcosms might be of special interest, as these reactions could effectively (albeit transiently) control accumulation of unwanted sulfides. Undoubtedly, there is a further need to establish that no other corrosive metabolites are being produced during the oxidation of sulfur species. Thiobacilli-like bacteria also were detected in MX-80 Batch 1 microcosms; however, it is possible that these were unable to out-compete the growing firmicute SRB, and they may not have had a sufficient supply of oxidized substrates to exceed sulfide production. Alternatively, proteobacterial SRB in Canapriil enrichments could have been inhibited by

sulfide or by other unidentified mechanisms (Maillacheruvu and Parkin, 1996), while Thiobacilli-like bacteria could be anticipated to periodically-sustain sulfide oxidation. The understanding of either reductive and oxidative sulfur metabolism in microbial populations is important from a corrosion perspective, because both pathways potentially could raise corrosion risks (Little et al., 2000) via production of sulfide (as discussed above, through the reduction of sulfur species) or by acidification of the aqueous phase (via oxidation of reduced sulfur compounds to ionized sulfuric acid). Finding no sulfide production in MX-80 Batch 2 enrichments was consistent with the molecular analyses of the microbial community that revealed no known SRB capable of producing sulfide present in their respective DNA libraries.

Looking to the functional competences within the respective microbial populations, it is noteworthy that for each gene family, PICRUSt reflects the known gene copy numbers (from complete sequenced genomes) onto a reference phylogenetic tree. These gene family copy numbers are treated as continuous traits, and an evolutionary model is constructed under the assumption of random rearrangement (i.e., Brownian motion). Therefore, the PICRUSt prediction is tentative in nature and its precision relies on the accuracy of reconstructed rRNA gene phylogenies and the availability of well-characterised whole genomes of phylogenetically-related microorganisms. In addition, our ranking methodology presents an additional uncertainty into the predictions. In addition to the expected predominance of purine metabolism, which is responsible for turnover of genetic materials, we observed a high abundance (top 10% of the predicted metagenome) in all microcosms of the following prokaryotic KEGG metabolic pathways (listed in decreasing order): oxidative phosphorylation; peptidases; metabolism of amino acids related enzymes, arginine and proline; carbon fixation pathways; pyruvate metabolism; methane metabolism; butanoate metabolism, propanoate metabolism, and glycolysis metabolism. The pathways associated with gaining energy, i.e., nitrogen metabolism, fatty acids metabolism, benzoate degradation, and aminobenzoate degradation were less abundant and represented 10–20% of the PICRUSt-predicted metagenome. An increased share of enzymes related to intracellular accumulation of the carbohydrate phosphate esters (phosphotransferase system), fructose and mannose metabolism, sporulation and peptidases in the sequenced 16S rRNA gene libraries from H_2 -fed microcosms with MX-80 Batch 1 clay, perhaps was due to enrichment of these incubations with spore-forming bacteria (e.g., *Bacillaceae*, *Peptostreptococcaceae*, *Clostridiaceae* and *Peptococcaceae*) that need these enzymatic systems for normal sporulation/germination processes (Bobek et al., 2014). Such an enrichment is of no coincidence since spore-formers have repeatedly been observed to predominate among cultivable bacteria in bentonites (Chi Fru and Athar, 2008; Gilmour et al., 2021; Grigoryan et al., 2020; Haynes et al., 2018; Jaliq et al., 2016; Matschiavelli et al., 2019; Podlech et al., 2021). The anoxic clay microcosms were highly likely driven primarily by sulfate and hydrogen, and the sulfur metabolism fell in the top 30–35% of the most significant contributor to metabolic processes. PICRUSt findings indicated a high proportion of bacteria able to catalyze a majority of reductive, as well as reverse – oxidative sulfur cycle reactions, in MX-80 Batch 1 and Canapriil clays, while enzymatic machinery for primarily oxidative sulfur cycling was indicated to exist in MX-80 Batch 2 enrichments.

From the 16S rRNA diversity in sequenced libraries, we can speculate that biogenic sulfidogenesis in clay microcosms could occur similarly to the sulfur cycling scenario observed in marine sediments, where 68–78% of the sulfide generated during bacterial sulfate-reduction is oxidized to thiosulfate (Jørgensen, 1990). Thiosulfate is then reduced back to sulfide, oxidized to sulfate and disproportionated to sulfide and sulfate via the thiosulfate shunt characteristic of anoxic sediments (Jørgensen, 1990). From a corrosion point of view, these metabolic cycles could be very important, as the interaction of thiosulfate and copper is much less studied than the copper-sulfide interaction, and there is some question about whether it may lead to copper cracking under physical loads (Bhaskaran et al., 2013; Taniguchi and Kawasaki, 2008). In MX-80 Batch 1 and

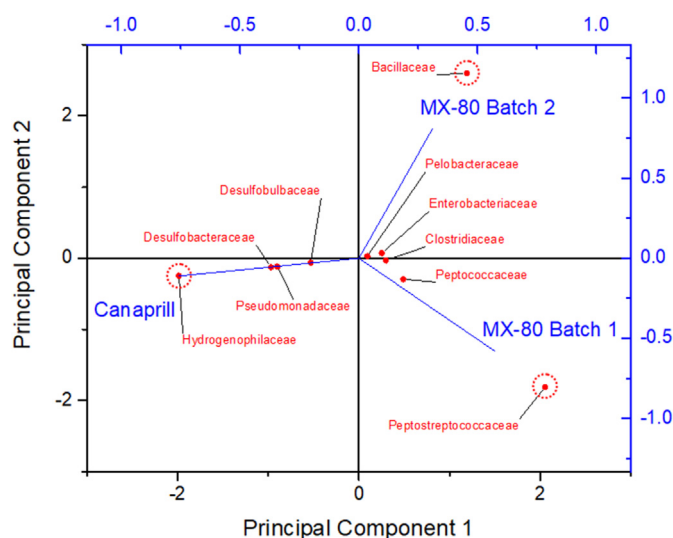


Figure 7. Principal component analysis (PCA) plots of the ranks of frequencies of top ten family-level OTUs that could putatively-contribute to biochemical reactions accelerating corrosion of metallic DGR materials. Dotted circles denote families that potentially represent a higher corrosion risk than other detected bacterial families.

Canapril microcosms, bacteria of families *Desulfobulbaceae*, *Peptococcaceae*, and *Desulfobacteraceae* possessed the enzymes responsible for subsequent reduction of sulfate to sulfide (Figure 4). As discussed, Thiobacilli-like bacteria of the family *Hydrogenophilaceae* might oxidize sulfide with the transient production of thiosulfate that, in turn, could be re-reduced to sulfide by putative thiosulfate reducers of the families *Clostridiaceae* (e.g., *Clostridium* spp.) and *Peptostreptococcaceae* (e.g., *Sedimentibacter* spp.). Bacteria of the family *Desulfobulbaceae* were also shown to catalyze sulfide oxidation to elemental sulfur under microaerobic conditions, followed by sulfur disproportionation to sulfate and sulfide (Fuseler and Cypionka, 1995). Additionally, some bacteria of the detected *Desulfuromonas-Pelobacter-Geobacter* group can reduce elemental sulfur to sulfide, thereby contributing to the total sulfide “pull”. Some bacteria in the families *Clostridiaceae*, *Peptostreptococcaceae* and *Veillonellaceae* also possess acetogenic capacity and if they are present and active, might facilitate reduction of sulfate to sulfide by sulfate- or thiosulfate-reducing microorganisms that require acetate for carbon assimilation (during reduction of electron acceptors coupled to oxidation of hydrogen) or that oxidize acetate (Figure 5). Recalcitrant hydrocarbons and products of their decomposition might be the only significant source of organic carbon for clay-based microbial populations (Grigoryan et al., 2018; Marshall et al., 2015). Therefore, the presence of the bacterial families *Pseudomonadaceae* and *Nocardiodaceae*, which routinely harbour genes for the decomposition of saturated hydrocarbons, and the family *Rhodocyclaceae* (e.g., *Magneto-spirillum* spp.), which frequently possesses enzymes for the degradation of aromatic hydrocarbons, could be critical for the sustained functioning of microbial consortia in clays. However, the availability of residual hydrocarbons and oxidants (i.e., oxygen, ferric iron or nitrate) for bacterial respiration in clays are expected to be low in a DGR for nuclear fuel waste. Thus, an abundance of hydrocarbon degrading microorganisms in clay enrichments would likely be of little importance, even though there were detectable DNA sequences present that suggest further transformation of hydrocarbons (e.g., via the β -oxidation pathway). Therefore, in these clay systems lacking organic carbon, the reductive synthesis of acetate would provide an indigenous microbial community with a readily-available carbon source required for bacterial growth, while concurrently exposing the surroundings to corrosive by-products. The ubiquitous distribution of hydrogenases responsible for initial H_2 -uptake (e.g., in bacteria of families *Peptostreptococcaceae*, *Clostridiaceae*, *Peptococcaceae*, *Hydrogenophilaceae*, *Desulfobacteraceae*, *Desulfobulbaceae* and *Pseudomonadaceae*) suggests that hydrogen would potentially be an important electron donor to drive the activity of a microbial population in clayish systems where a shortage of complex organic compounds exists. For deep underground environments deficient in organics, such as a DGR for high level nuclear waste, subsurface hydrogen gas generated as a result of radiolysis of water and/or anaerobic metal corrosion could be a key factor in the development of a microbial community (Bagnoud et al., 2016). As discussed earlier, similar H_2 -scavenging enzymes may participate in material corrosion reactions. However, the kinetics of H_2 -uptake in both biochemical and corrosion reactions are still unclear and need to be described quantitatively.

The 16S rRNA gene diversity discovered in water-saturated low-density MX-80 Batch 1 microcosms (Grigoryan et al., 2018, 2020; Svensson et al., 2011, and the current study) resembles those of bacterial populations detected within highly-compacted bentonites (Chi Fru and Athar, 2008; Grigoryan et al., 2020; Hallbeck et al., 2017; Jaliq et al., 2016; Svensson et al., 2011). In a recent study, Povedano-Priego et al. (2021) developed refined methods for improving DNA yields for amplicon sequence analysis from indigenous microbes inhabiting highly-compacted clays. Using compacted (1.5 and 1.7 gr/cm³), acetate-amended bentonite clay incubated for 24 months as a model system, the authors detected bacterial taxa that included both oxidizers and reducers of sulfur and iron, as well as organisms that could utilize acetate. It has long been recognized that clay-based systems are challenging materials from which to recover microbial DNA. Therefore, microbiological insights derived from uncompacted clay microcosms

can, to some extent, be representative of a DGR environment as well, and offer some advantage in terms of extracting nucleic acids from microbes that have managed to increase in number due to lack of typical constraints seen under high swelling pressure, low pore space and low water availability in highly compacted clay (Jaliq et al., 2016). Others found bacteria of the *Desulfuromonas-Pelobacter-Geobacter* group, along with some bacteria within the *Desulfovibrionaceae*, were detected using either DGGE (Grigoryan et al., 2018; Svensson et al., 2011) or high throughput sequencing in clay microcosms or enrichments (Gilmour et al., 2021; Grigoryan et al., 2018; Haynes et al., 2018, and the current study) and in biofilms associated with compacted bentonites (Hallbeck et al., 2017). It has been speculated recently that these bacteria, may be capable of harvesting electrons for sulfoxyanion reduction directly from insoluble minerals and metals using several extracellular multi-heme cytochromes (Deng et al., 2018), and therefore causing their corrosion. However, it is unclear whether clays can serve as selective substrates that facilitate enrichment of bacteria directly using electrons from solids, similar to iron specimens, which have earlier facilitated enrichment and isolation of these kinds of microorganisms (Dinh et al., 2004).

The functional roles of *Chloroflexi* (*Anaerolineaceae*) detected in MX-80 Batch 1 and MX-80 Batch 2 enrichments remains unclear. It is not surprising that these clay samples share bacteria of the same phylum, since these clay products most likely originated from similar outcrops. Bacteria of the phylum *Chloroflexi* occur in subsea sediments, deep geological formations and pipe-associated brackish waters (Blazejak and Schippers, 2010; Fowler et al., 2016; Fry et al., 2008; Park et al., 2011). Microorganisms of that taxon might participate in hydrocarbon transformation, i.e., *Anaerolineaceae* in sulfidic natural hydrocarbon seeps have been shown to metabolise short-chain, low-molecular-weight alkanes under mesophilic, sulfate-reducing conditions (Savage et al., 2010). Extensive hydrocarbon decomposition was also evident under sulfate-reducing conditions with 77% removal of alkanes in 300 days by oil-degrading microcosms inoculated with River Tyne estuarine sediments with sequences from the phylum *Chloroflexi* (*Anaerolineaceae* spp.) being most frequently encountered (24%), together with Firmicutes (20%) and Deltaproteobacteria (19%) (Sherry et al., 2013). This could suggest that bacteria of the phylum *Chloroflexi* could contribute to the decomposition of recalcitrant hydrocarbons and stimulate total carbon turnover in clay microcosms. Yet, all these observations are of an exploratory nature in our case, because the majority sequences discovered in the current study were phylogenetically-distinct from bacteria of known physiology.

In order to evaluate bacteria (or to be more accurate, OTUs) in clay microcosms based on corrosion risks that they can potentially represent, we described them in terms of the prevalence of genes encoding corrosion-related functionalities in predicted metagenomes and frequencies of OTUs that potentially harbour corrosion-related functionalities. This approach is expected to help in identifying high corrosion-risk bacteria among diverse microbial populations. Thus, sorting out bacteria of families of *Peptostreptococcaceae*, *Hydrogenophilaceae*, *Bacillaceae*, as well as *Peptococcaceae*, *Clostridiaceae*, *Enterobacteriaceae*, *Pelobacteraceae*, *Pseudomonadaceae*, *Desulfobacteraceae* and *Desulfobulbaceae* as potential contributors to material corrosion was based on their relatively high abundances in microcosms and on their easy-recruitable diversified metabolic pathways-of-interest (i.e., ability to take part in corrosive hydrogen uptake, acid production and sulfur cycling). As has already been mentioned, the use of hydrogen-fed microcosms triggered enrichment of these corrosion-related metabolic pathways. Though microbial populations under DGR conditions will likely be less abundant and have a different taxonomic distribution, the microcosm model that has been applied in the current study might still assist in identifying potentially high-risk bacteria and offer development of targeted solutions for their control.

5. Conclusions

Hydrogen-fed clay microcosms can be useful models for enrichment of microorganisms from commercial bentonites where transient growth

in a DGR under continuous influx of H₂ would be anticipated to occur at low-density water saturated interfaces (Stroes-Gascoyne et al., 2010). Enrichment of bacteria from three different clays resulted in the slow development of three dissimilar microbial populations capable of sustaining themselves under the imposed conditions in this study. Sulfidogenic activity was observed only in two of the three types of microcosms, i.e., those containing MX-80 Batch 1 and Canapril. The pattern of sulfide production in these microcosms was fashioned by the enriched microbial populations. For instance, in the MX-80-based systems, a relatively homogeneous microbial community composed mainly of (based on the 16S rRNA gene PICRUSt analysis) the phyla Firmicutes and Chloroflexi, with fermentative (i.e., *Clostridiaceae* spp. and *Anaerolineaceae* spp.) or sulfate-reducing (i.e., *Desulfosporosinus* spp.) metabolism, a concentration of >3.5 mM sulfide was accumulated progressively. Canapril microcosms developed a more diverse community where the majority of sequences were related to sulfate-reducing bacteria of the family *Desulfobulbaceae*, although sequences related to taxa capable of oxidizing sulfide/sulfur were also detected. Consequently, the accumulation of sulfide in Canapril microcosms attributed to SRB activity was transient and appeared to be reversed periodically, possibly by sulfide oxidation by Thiobacilli-like microorganisms. Based on a PICRUSt-predicted distribution of gene families, it was hypothesized that growth of SRB was sustained through direct hydrogen uptake by hydrogenases in SRB and through the activity of acetogenic bacteria (of the families *Clostridiaceae* and *Peptostreptococcaceae*), that produced acetate from H₂ and CO₂ which subsequently served as a readily available (catabolic or anabolic) carbon source for other microorganisms. Similar sulfidogenic and acetogenic bacteria of the families *Peptococcaceae*, *Desulfobulbaceae*, *Desulfobacteraceae*, *Clostridiaceae*, and *Peptostreptococcaceae* would pose a corrosion risk in these microcosms (Figure 7); however, the actual corrosion rates involved in these processes remains to be determined. The capability of clay microcosms to support microbial growth via the decomposition of residual hydrocarbons is believed to be limited overall, due to the shortage of organics in clay (Marshall et al., 2015) along with the relatively low abundance of primary degraders (i.e., *Pseudomonadaceae* sp.). Although the analysis of the 16S rRNA gene libraries by PICRUSt scripts in this study allows functional profiling of the microbial populations that were enriched, a shotgun metagenomic approach that amplifies all genes present could provide a more reliable assessment if reasonable member coverage were available, and could then be followed ideally by metatranscriptomic-based analysis of *in situ* gene expression.

It should be emphasized that the results of the microcosm experiments are not directly applicable to intact barriers in a DGR due to the very limited and suppressed microbial activity found in such highly-compacted bentonite environments. However, the results of this study may be relevant to regions in a DGR where the bentonite is poorly emplaced, and consequently where bentonite density loss has been caused by phenomena such as piping and colloid formation, or during initial wetting of the barrier system where the bentonite clay hasn't undergone full expansion/swelling. The careful design and construction of bentonite-based barriers could conceivably prevent the occurrence of such troublesome regions.

Declarations

Author contribution statement

Alexander A. Grigoryan: Conceived and designed the experiments; Performed the experiments; Analyzed and interpreted the data; Wrote the paper.

Daphne R. Jalique, Peter G. Keech: Analyzed and interpreted the data; Wrote the paper.

Simcha Stroes-Gascoyne: Conceived and designed the experiments; Analyzed and interpreted the data; Wrote the paper.

Gideon M. Wolfardt, Darren R. Korber: Conceived and designed the experiments; Analyzed and interpreted the data; Contributed reagents, materials, analysis tools or data; Wrote the paper.

Funding statement

This work was supported by the Nuclear Waste Management Organization (Canada) and the Natural Sciences and Engineering Research Council of Canada (NSERC) Collaborative Research and Development Grant to DRK/GMW.

Data availability statement

Data associated with this study has been deposited at NCBI Sequence Read Archive under the accession number PRJNA719485.

Competing interest statement

The authors declare no conflict of interest.

Additional information

No additional information is available for this paper.

Acknowledgements

Special thanks to Dr. Natallia Varankovich of the University of Saskatchewan for technical assistance during preparation of the 16S rRNA gene libraries and DNA sequencing. We also wish to acknowledge Amec Foster Wheeler plc (United Kingdom) for providing samples of the MX-80 Batch 2 bentonite.

References

- Aßhauer, K.P., Wemheuer, B., Daniel, R., Meinicke, P., 2015. Tax4Fun: predicting functional profiles from metagenomic 16S rRNA data: Fig 1. *Bioinformatics* 31 (17).
- Bagnoud, A., Chourey, K., Hettich, R.L., de Bruijn, L., Andersson, A.F., Leupin, O.X., Schwyn, B., Bernier-Latmani, R., 2016. Reconstructing a hydrogen-driven microbial metabolic network in Opalinus Clay rock. *Nat. Commun.* 7 (1).
- Bhaskaran, G., Carcea, A., Ulaganathan, J., Wang, S., Huang, Y., Newman, R.C., 2013. Fundamental Aspects of Stress Corrosion Cracking of Copper Relevant to the Swedish Deep Geologic Repository Concept. SKB Technical Report. SKB-TR-12-06. <http://www.skb.se/upload/publications/pdf/TR-12-06.pdf>.
- Blasco-Gómez, Ramiro, Battle-Vilanova, Pau, Villano, Marianna, Balaguer, Maria Dolores, Colprim, Jesús, Puig, Sebastià, 2017. On the edge of research and technological application: a critical review of electromethanogenesis. *Int. J. Mol. Sci.* 18, 874.
- Blazejak, A., Schippers, A., 2010. High abundance of JS-1- and *Chloroflexi*-related *Bacteria* in deeply buried marine sediments revealed by quantitative, real-time PCR. *FEMS Microbiol. Ecol.* 72 (2).
- Bobek, J., Strakova, E., Zikova, A., Vohradsky, J., 2014. Changes in activity of metabolic and regulatory pathways during germination of *S. coelicolor*. *BMC Genom.* 15 (1).
- Bomberg, M., Lamminmäki, T., Itävaara, M., 2016. Microbial communities and their predicted metabolic characteristics in deep fracture groundwaters of the crystalline bedrock at Olkiluoto, Finland. *Biogeosciences* 13 (21).
- Bryant, R.D., Jansen, W., Boivin, J., Laishley, E.J., Costerton, J.W., 1991. Effect of hydrogenase and mixed sulfate-reducing bacterial populations on the corrosion of steel. *Appl. Environ. Microbiol.* 57 (10).
- Bryant, R.D., Laishley, E.J., 1990. The role of hydrogenase in anaerobic biocorrosion. *Can. J. Microbiol.* 36 (4).
- Caporaso, J.G., Kuczynski, J., Stombaugh, J., Bittinger, K., Bushman, F.D., Costello, E.K., Fierer, N., Peña, A.G., Goodrich, J.K., Gordon, J.I., Huttley, G.A., Kelley, S.T., Knights, D., Koenig, J.E., Ley, R.E., Lozupone, C.A., McDonald, D., Muegge, B.D., Pirrung, M., Knight, R., 2010. QIIME allows analysis of high-throughput community sequencing data. *Nat. Methods* 7 (5).
- Chi Fru, E., Athar, R., 2008. In situ bacterial colonization of compacted bentonite under deep geological high-level radioactive waste repository conditions. *Appl. Microbiol. Biotechnol.* 79 (3).
- Chong, Grace, Karbelkar, Amruta, El-Naggar, Mohamed, 2018. Nature's conductors: What can microbial multi-heme cytochromes teach us about electron transport and biological energy conversion? *Curr. Opin. Chem. Biol.* 47, 7–17.
- de Silva Muñoz, L., Bergel, A., Basséguy, R., 2007. Role of the reversible electrochemical deprotonation of phosphate species in anaerobic biocorrosion of steels. *Corrosion Sci.* 49 (10).
- Deng, X., Dohmae, N., Neelson, K.H., Hashimoto, K., Okamoto, A., 2018. Multi-heme cytochromes provide a pathway for survival in energy-limited environments. *Sci. Adv.* 4 (2).

- Deutzmann, J.S., Sahin, M., Spormann, A.M., 2015. Extracellular enzymes facilitate electron uptake in biocorrosion and bioelectrosynthesis. *mBio* 6 (2).
- Dinh, H.T., Kuever, J., Mußmann, M., Hassel, A.W., Stratmann, M., Widdel, F., 2004. Iron corrosion by novel anaerobic microorganisms. *Nature* 427 (6977).
- Drake, H.L., Küsel, K., Matthies, C., 2013. Acetogenic prokaryotes. In: *The Prokaryotes: Prokaryotic Physiology and Biochemistry*.
- Enning, D., Garrelfs, J., 2014. Corrosion of iron by sulfate-reducing bacteria: new views of an old problem. *Appl. Environ. Microbiol.* 80 (4).
- Fowler, S.J., Toth, C.R.A., Gieg, L.M., 2016. Community structure in methanogenic enrichments provides insight into syntrophic interactions in hydrocarbon-impacted environments. *Front. Microbiol.* 7 (APR).
- Fry, J.C., Parkes, R.J., Cragg, B.A., Weightman, A.J., Webster, G., 2008. Prokaryotic biodiversity and activity in the deep seafloor biosphere. *FEMS Microbiol. Ecol.* 66 (2).
- Fuseler, K., Cypionka, H., 1995. Elemental sulfur as an intermediate of sulfide oxidation with oxygen by *Desulfobulbus propionicus*. *Arch. Microbiol.* 164 (2).
- Gilmour, K.A., Davie, C.T., Gray, N., 2021. An indigenous iron-reducing microbial community from MX80 bentonite - a study in the framework of nuclear waste disposal. *Appl. Clay Sci.* 205.
- Grigoryan, A., Jalique, D.R., Medihala, P., Stroes-Gascoyne, S., Wolfaardt, G.M., McKelvie, J., Korber, D.R., 2018. Bacterial diversity and production of sulfide in microcosms containing uncompact bentonites. *Heliyon* 4 (8).
- Grigoryan, A., Stroes-Gascoyne, S., Jalique, D.R., Wolfaardt, G.M., Keech, P., McKelvie, J., Korber, D.R., 2020. Baseline Distribution and Diversity of MIC-Relevant Microorganisms in Compacted Bentonites after Incubation for 1 Year. NACE - International Corrosion Conference Series.
- Hallbeck, L., Johansson, L., Edlund, J., Pedersen, K., 2017. Microbial Analyses of Groundwater, Bentonite and Surfaces-Post-test Analysis of Packages 4 (A05) and 5 (A06) from the MiniCan Experiment. SKB Technical Report. TR-16-13. www.skb.com/publication/2488209/TR-16-13.pdf.
- Haynes, H.M., Pearce, C.I., Boothman, C., Lloyd, J.R., 2018. Response of bentonite microbial communities to stresses relevant to geodisposal of radioactive waste. *Chem. Geol.* 501.
- Herlemann, D.P.R., Labrenz, M., Jürgens, K., Bertilsson, S., Waniek, J.J., Andersson, A.F., 2011. Transitions in bacterial communities along the 2000 km salinity gradient of the Baltic Sea. *ISME J.* 5 (10).
- Jalique, D.R., Stroes-Gascoyne, S., Hamon, C.J., Priyanto, D.G., Kohle, C., Evenden, W.G., Wolfaardt, G.M., Grigoryan, A.A., McKelvie, J., Korber, D.R., 2016. Culturability and diversity of microorganisms recovered from an eight-year old highly-compacted, saturated MX-80 Wyoming bentonite plug. *Appl. Clay Sci.* 126.
- Jørgensen, B.B., 1990. A thiosulfate shunt in the sulfur cycle of marine sediments. *Science* 249 (4965).
- Jun, S.R., Robeson, M.S., Hauser, L.J., Schadt, C.W., Gorin, A.A., 2015. PanFP: pangenome-based functional profiles for microbial communities. *BMC Res. Notes* 8 (1).
- Kanehisa, M., Goto, S., Sato, Y., Furumichi, M., Tanabe, M., 2012. KEGG for integration and interpretation of large-scale molecular data sets. *Nucleic Acids Res.* 40 (D1).
- King, F., 2009. Microbiologically influenced corrosion of nuclear waste containers. *Corrosion* 65 (4).
- King, F., 2013. Container materials for the storage and disposal of nuclear waste. *Corrosion* 69 (10).
- Kouzuma, Atsushi, Ishii, Shun 'ichi, Watanabe, Kazuya, 2018. Metagenomic insights into the ecology and physiology of microbes in bioelectrochemical systems. *Biores. Technol.* 255, 302–307.
- Kryachko, Y., Hemmingsen, S.M., 2017. The role of localized acidity generation in microbially influenced corrosion. *Curr. Microbiol.* 74 (7).
- Langille, M.G.I., Zaneveld, J., Caporaso, J.G., McDonald, D., Knights, D., Reyes, J.A., Clemente, J.C., Burkepille, D.E., Vega Thurber, R.L., Knight, R., Beiko, R.G., Huttenhower, C., 2013. Predictive functional profiling of microbial communities using 16S rRNA marker gene sequences. *Nat. Biotechnol.* 31 (9).
- Little, B.J., Ray, R.I., Pope, R.K., 2000. Relationship between corrosion and the biological sulfur cycle: a review. *Corrosion* 56 (4).
- Magoč, T., Salzberg, S.L., 2011. FLASH: fast length adjustment of short reads to improve genome assemblies. *Bioinformatics* 27 (21).
- Maillacheruvu, K.Y., Parkin, G.F., 1996. Kinetics of growth, substrate utilization and sulfide toxicity for propionate, acetate, and hydrogen utilizers in anaerobic systems. *Water Environ. Res.* 68 (7).
- Markowitz, V.M., Chen, I.M.A., Chu, K., Szeto, E., Palaniappan, K., Grechkin, Y., Ratner, A., Jacob, B., Pati, A., Huntemann, M., Liolios, K., Pagani, I., Anderson, I., Mavromatis, K., Ivanova, N.N., Kyrpides, N.C., 2012. IMG/M: the integrated metagenome data management and comparative analysis system. *Nucleic Acids Res.* 40 (D1).
- Marshall, M.H.M., McKelvie, J.R., Simpson, A.J., Simpson, M.J., 2015. Characterization of natural organic matter in bentonite clays for potential use in deep geological repositories for used nuclear fuel. *Appl. Geochem.* 54.
- Matschiavelli, N., Kluge, S., Podlech, C., Standhaft, D., Grathoff, G., Ikeda-Ohno, A., Warr, L.N., Chukharkina, A., Arnold, T., Cherkouk, A., 2019. The year-long development of microorganisms in uncompact bavarian bentonite slurries at 30 and 60 °C. *Environ. Sci. Technol.* 53 (17).
- McDonald, D., Price, M.N., Goodrich, J., Nawrocki, E.P., Desantis, T.Z., Probst, A., Andersen, G.L., Knight, R., Hugenholtz, P., 2012. An improved Greengenes taxonomy with explicit ranks for ecological and evolutionary analyses of bacteria and archaea. *ISME J.* 6 (3).
- Mehanna, M., Basseguy, R., Delia, M.L., Bergel, A., 2009. Role of direct microbial electron transfer in corrosion of steels. *Electrochem. Commun.* 11 (3).
- Mehanna, M., Basseguy, R., Delia, M.L., Girbal, L., Demuez, M., Bergel, A., 2008. New hypotheses for hydrogenase implication in the corrosion of mild steel. *Electrochim. Acta* 54 (1).
- Park, H.S., Chatterjee, I., Dong, X., Wang, S.H., Sensen, C.W., Caffrey, S.M., Jack, T.R., Boivin, J., Voordouw, G., 2011. Effect of sodium bisulfite injection on the microbial community composition in a brackish-water-transporting pipeline. *Appl. Environ. Microbiol.* 77 (19).
- Pfennig, N., Lippert, K.D., 1966. Über das vitamin B 12-bedürfnis phototropher Schwefelbakterien. *Arch. Mikrobiol.* 55 (3).
- Podlech, C., Matschiavelli, N., Peltz, M., Kluge, S., Arnold, T., Cherkouk, A., Meleshyn, A., Grathoff, G., Warr, L.N., 2021. Bentonite alteration in Batch reactor experiments with and without organic supplements: implications for the disposal of radioactive waste. *Minerals* 11 (9).
- Pope, D.H., Zintel, T.P., Kuruvilla, A.K., Siebert, O.W., 1988. organic acid corrosion of carbon steel: a mechanism of microbiologically influenced corrosion. *Corrosion* 88.
- Povedano-Priego, C., Jroundi, F., Lopez-Fernandez, M., Shrestha, R., Spanek, R., Martín-Sánchez, I., Villar, M.V., Ševců, A., Dopson, M., Merroun, M.L., 2021. Deciphering indigenous bacteria in compacted bentonite through a novel and efficient DNA extraction method: insights into biogeochemical processes within the Deep Geological Disposal of nuclear waste concept. *J. Hazard Mater.* 408.
- Rabus, R., Venceslau, S.S., Wöhlbrand, L., Voordouw, G., Wall, J.D., Pereira, I.A.C., 2015. A post-genomic view of the ecophysiology, catabolism and biotechnological relevance of sulphate-reducing prokaryotes. In: *Advances in Microbial Physiology*, 66.
- Rajala, P., Bomberg, M., Vepsäläinen, M., Carpen, L., 2017. Microbial fouling and corrosion of carbon steel in deep anoxic alkaline groundwater. *Biofouling* 33 (2).
- Savage, K.N., Krumholz, L.R., Gieg, L.M., Parisi, V.A., Suflita, J.M., Allen, J., Philp, R.P., Elshahed, M.S., 2010. Biodegradation of low-molecular-weight alkanes under mesophilic, sulfate-reducing conditions: metabolic intermediates and community patterns. *FEMS Microbiol. Ecol.* 72 (3).
- Sherry, A., Gray, N.D., Ditchfield, A.K., Aitken, C.M., Jones, D.M., Röling, W.F.M., Hallmann, C., Larter, S.R., Bowler, B.F.J., Head, I.M., 2013. Anaerobic biodegradation of crude oil under sulphate-reducing conditions leads to only modest enrichment of recognized sulphate-reducing taxa. *Int. Biodeterior. Biodegrad.* 81.
- Silva, D., Basséguy, R., Bergel, A., 2002. The role of hydrogenases in the anaerobic microbiologically influenced corrosion of steels. *Bioelectrochemistry* 56 (1–2).
- Spiegelman, D., Whissell, G., Greer, C.W., 2005. A survey of the methods for the characterization of microbial consortia and communities. *Can. J. Microbiol.* 51 (Issue 5).
- Stroes-Gascoyne, S., Hamon, C.J., Maak, P., Russell, S., 2010. The effects of the physical properties of highly compacted smectitic clay (bentonite) on the culturability of indigenous microorganisms. *Appl. Clay Sci.* 47 (1–2).
- Svensson, D., Dueck, A., Nilsson, U., Olsson, S., Sandén, T., Lydmark, S., Jägerwall, S., Pedersen, K., Hansen, S., 2011. Alternative Buffer Material. Status of the Ongoing Laboratory Investigation of Reference Materials and Test Package 1. SKB Technical Report. TR-11-06. <http://www.skb.se/upload/publications/pdf/TR-11-06.pdf>.
- Taniguchi, N., Kawasaki, M., 2008. Influence of sulfide concentration on the corrosion behavior of pure copper in synthetic seawater. *J. Nucl. Mater.* 379 (1–3).
- Trüper, H.G., Schlegel, H.G., 1964. Sulphur metabolism in Thiorhodaceae I. Quantitative measurements on growing cells of *Chromatium okenii*. *Antonie Leeuwenhoek* 30 (1).
- Villagran, J., ben Belfadhel, M., Birch, K., Freire-Canosa, J., Garamszeghy, M., Garisto, F., Gierszewski, P., Gobien, M., Hirschorn, S., Hunt, N., Khan, A., Kremer, E., Kwong, G., Lam, T., Maak, P., McKelvie, J., Medri, C., Murchison, A., Russell, S., Yang, T., 2011. RD&D Program 2011 – NWMO's Program for Research, Development and Demonstration for Long-Term Management of Used Nuclear Fuel. NWMO Technical Report. TR-2011-01.
- Widdel, F., Bak, F., 1992. Gram-negative mesophilic sulfate-reducing bacteria. In: *The Prokaryotes*.
- Zeikus, J.G., Weimer, P.J., Nelson, D.R., Daniels, L., 1975. Bacterial methanogenesis: acetate as a methane precursor in pure culture. *Arch. Microbiol.* 104 (1).